

Multi-Frame, Lightweight & Efficient Vision-Language Models for Question Answering in Autonomous Driving

Anonymous CVPR submission

Paper ID 8

Abstract

Vision-Language Models (VLMs) and Multi-Modal Language Models (MMLMs) have become prominent in autonomous driving research, as these models can provide interpretable textual reasoning and responses for end-to-end autonomous driving safety tasks using traffic scene images and other data modalities. However, current approaches to these systems use expensive large language model (LLM) backbones and image encoders, making such systems unsuitable for real-time autonomous driving systems where tight memory constraints exist and fast inference time is necessary. To address these previous issues, we develop EM-VLM4AD, an efficient, lightweight, multi-frame vision language model which performs Visual Question Answering for autonomous driving. In comparison to previous approaches, EM-VLM4AD requires at least 10 times less memory and floating point operations, while also achieving higher BLEU-4, METEOR, CIDEr, and ROGUE scores than the existing baseline on the DriveLM dataset. EM-VLM4AD also exhibits the ability to extract relevant information from traffic views related to prompts and can answer questions for various autonomous driving subtasks. We release our code to train and evaluate our model [here](#).

1. Introduction

Vision-Language Models (VLMs) have emerged as powerful tools that possess holistic knowledge to solve tasks at the intersection of vision and language. This makes them a promising asset in autonomous driving (AD), allowing for a driver to interact with the VLM which can provide interpretable language representations of various driving safety tasks. Furthermore, VLMs can serve as end-to-end autonomous driving systems, eliminating integration and propagating errors between separate models specializing in specific sub-tasks of autonomous driving such as perception [14–16] and trajectory planning [25]. These potential benefits have propelled the development of many vision-

language models and multimodal language models tailored for autonomous driving applications [5, 24, 31, 32, 38]. These models cover various aspects of autonomous driving including closed-loop control, perception tasks, and traffic agent behavior analysis.

Typically, the process in a VLM is the following: vision and text features are encoded separately, then fused together through a concatenation or projection layer, and then finally fed into an LLM to output some probability distribution over the vocabulary [37]. While generating text embeddings is relatively low-cost, the LM and image embeddings can often entail high computational costs. In real-time systems such as autonomous driving, prioritizing the development of VLMs with efficient inference times is crucial for practical deployment in vehicles. However, current research in applying multimodal language models to autonomous driving predominantly use large models such as BLIP-2 [20], GPT 3.5 [24], and LLaMA-7b [32], all of which contain over one billion parameters. Consequently, these models require expensive hardware and longer inference times, limiting their potential to be applied in current vehicles and accessibility for researchers with limited computational resources.

This paper focuses on the development of lightweight vision-language models with less than one billion parameters than can accurately and efficiently answer questions related to autonomous driving safety tasks. We develop the model EM-VLM4AD: Efficient, Multi-Frame Vision-Language Model for Autonomous Driving. We use the DriveLM dataset [31], which offers real, multi-view traffic scene images paired with question/answer pairs to train this model. Our contributions are as follows:

- We develop an efficient, smaller vision-language model EM-VLM4AD that consumes at least **10x** less memory and floating point operations (FLOPs) than current AD-VLMs, and can also respond to questions conditioned on multiple frames.
- We explore two different lightweight LM backbones for EM-VLM4AD: a finetuned Text-to-Text Transfer Transformer (T5) Base LM and an 8-bit quantized T5-Large LM finetuned using low-rank adaptation (LoRA) [18].

076 • We compare our model efficiency and performance on
077 BLEU-4 (Bilingual Evaluation Understudy), CIDEr
078 (Consensus-based Image Description Evaluation),
079 ROUGE-L (Recall-Oriented Understudy for Gisting
080 Evaluation), and METEOR (Metric for Evaluation of
081 Translation with Explicit Ordering) to the baseline
082 for the DriveLM dataset [31], demonstrating stronger
083 performance in all metrics even with superior efficiency
084 using a much smaller model.

085 2. Related Research

086 2.1. Vision-Language Models

087 Initially designed to operate on sequence data, Transform-
088 ers [33] achieved state-of-the-art performance for natural
089 language processing tasks. This propelled the develop-
090 ment of Large Language Models, which learn general sta-
091 tistical properties of language through pretraining Encoder
092 [9], Encoder-Decoder [29], and Decoder [2, 27, 32] Trans-
093 former architectures on a large corpus of tokens. These pre-
094 trained models can then be finetuned for downstream, more
095 specialized language tasks. Dosovitskiy et al. [10] intro-
096 duced the application of Transformers to image tasks with
097 the Vision Transformer (ViT), which converts images into
098 a sequence representation of image patches that can be pro-
099 cessed by Transformers. Vision-Language Models bridge
100 the gap between LLMs and Vision Transformers, encod-
101 ing images and text into a combined latent representation
102 and then utilizing cross-modal pre-training tasks to learn
103 text and image correlations. This general approach to mul-
104 timodal learning has sparked a variety of vision-language
105 models. Radford et al. [28] devise a pre-training task of
106 matching text captions with images to develop CLIP, which
107 learns state-of-the-art image representations and exhibits
108 strong zero-shot transfer capabilities for many image classi-
109 fication tasks. BLIP-2 [20] introduces a two stage pretrain-
110 ing process to train a Querying Transformer “QFormer” that
111 serves as a intermediary between a frozen image encoder
112 and language model. This approach outperforms much
113 larger vision-language models such as Flamingo [1] and
114 is capable of zero-shot image-to-text generation. Instruct-
115 BLIP [7] builds off BLIP-2 and is a general-purpose VLM
116 that aggregates public vision-language datasets and trans-
117 forms them into an instruction tuning format. The VLM
118 most similar to the model introduced in this paper is VL-
119 T5 [6], which extends a pre-trained T5 to learn to generate
120 text labels conditioned on a combination of a text and im-
121 age embedding. Using a pre-trained LLM as a framework
122 for multi-modal tasks harnesses the text generation ability
123 of these models, critical for the question-answering task
124 in our research. Despite their strong performance across
125 many tasks, deploying these large models, which often ex-
126 ceed one billion parameters, is difficult for real-time appli-

cations [11]. Consequently, researching compression tech-
127 niques like distillation [12, 21], quantization, and pruning is
128 imperative to reduce VLM latency and computational costs. 129

2.2. Multimodal LLMs for Autonomous Driving 130

131 While autonomous driving systems mainly use visual fea-
132 tures, introducing linguistic features can enhance the inter-
133 pretability of these systems and even help identify novel
134 traffic situations [13]. This benefit has sparked research in-
135 terest in integrating multimodal data to train language mod-
136 els to become autonomous driving agents. Chen et al. [5]
137 design an architecture that fuses vectorized numeric modal-
138 ities with a pretrained LLaMA-7b [32] to solve Driving
139 Question Answering tasks. Using a two-step training ap-
140 proach, they initially ground the vector representations into
141 interpretable embeddings for the frozen LLaMA model, fol-
142 lowed by finetuning the LLM with LoRA [18]. DriveGPT4
143 [38] also adopts LLaMA as a backbone LLM and CLIP as
144 a visual encoder, using a traffic scene video and prompt text
145 as input to generate answers and low-level vehicle control
146 signals. To expand off the fixed and rigid QA labels from
147 the BDD-X dataset [19], DriveGPT4 is trained on instruc-
148 tion tuning data generated by ChatGPT/GPT4. DriveGPT4
149 only uses a single-view camera, which restricts it to ques-
150 tions involving a single view. Wang et al. [35] introduce
151 DriveMLM, which uses multi-view images, LiDAR Point
152 Clouds, traffic rules, and user commands from a realistic
153 simulator to perform closed-loop driving. This multimodal
154 model is built from LLaMA-7B and ViT-g/14 as the image
155 processor. Sha et al. [30] devise a chain-of-thought [36]
156 framework for driving scenarios using ChatGPT 3.5 to pro-
157 vide interpretable, logical reasoning for autonomous driving
158 systems. Mao et al. [24] also leverage the GPT-3.5 model
159 to create a motion planner for autonomous vehicles. Their
160 model, GPT-Driver, reformulates motion planning as a lan-
161 guage modeling problem by representing planner inputs and
162 outputs as language tokens. Recently, Sima et al. [31] re-
163 leased the DriveLM dataset, a Graph Visual Question An-
164 swering dataset that provides question-answer pairs related
165 to perception, behavior, and ego-vehicle planning based off
166 multi-view image data from the NuScenes dataset [4]. To
167 introduce a baseline, Sima et al. finetune BLIP-2 [20] for
168 this novel dataset.

169 While these approaches provide valuable explainability
170 for AD systems and exhibit strong performance for end-to-
171 end tasks, all these models use LLMs with over one billion
172 parameters (GPT 3.5, LLaMA, etc.) and expensive image
173 encoders like CLIP and ViT-g/14. This makes them primar-
174 ily suitable for offline scenarios where latency is not a pri-
175 ority, but not for online situations where real-time inference
176 is paramount.

177 2.3. Multi-Image Vision-Language Models

178 In the realm of autonomous driving, modalities beyond text
179 and image such as LiDAR, radar, or video offer important
180 features for many downstream tasks. However, most vision-
181 language models are pre-trained for single-image single-
182 text problems, making it unfeasible to directly input mul-
183 tiple images or modalities with a piece of text [37]. Con-
184 sequently, it is necessary to consolidate multiple modalities
185 and text into a single embedding that can be used by
186 a VLM. DriveGPT4 [38] encodes video input by pooling
187 CLIP visual encodings of each video frame. DriveMLM’s
188 [31] multimodal tokenizer uses QFormer to embed video
189 and LiDAR data, and then concatenates these embeddings
190 with text and system message embeddings. Wu et al. [37]
191 find that using gated attention pooling across each individ-
192 ual image embedding helps introduce more non-linearity
193 and extracts visual information across multiple images. Im-
194 portantly, this gated attention method introduces a negligi-
195 ble amount of computational overhead, rendering it an ideal
196 choice for our model to aggregate multi-view traffic scene
197 images into a unified embedding.

198 3. Methods

199 Our model for Visual Question Answering (VQA) in Au-
200 tonomous Driving, EM-VLM4AD, consists of a custom
201 image embedding network and a pre-trained T5 language
202 model [29]. We describe these following modules and the
203 overall training process in this section.

204 3.1. Image Embedding Network

205 To tackle multi-view (Front, Front-Left, Front-Right, Back,
206 Back-Left, Back-Right) QA tasks for autonomous driving,
207 individual image embeddings need to be aggregated into a
208 single embedding. This unified embedding can then be con-
209 catenated with a text embedding to serve as input to the LM.
210 In typical VLMs, the image embedding process uses models
211 like CLIP or object detection networks, resulting in a slow
212 extraction process. To address this, we adopt the patch pro-
213 jection embedding scheme introduced by ViT [10]. Given
214 an RGB image $I \in \mathbb{R}^{3 \times H \times W}$, the images are flattened
215 and sliced into patches with a linear projection and posi-
216 tional embedding. This creates a latent image representa-
217 tion $V_i \in \mathbb{R}^{S_I \times H_I}$, where S_I is the sequence length for the
218 image embedding and H_I is the hidden dimension of the
219 image embedding. We use the pretrained weights of ViT-
220 B/32 pretrained on ImageNet [8] to generate these image
221 embeddings.

222 This leaves us with 6 distinct individual image embed-
223 dings from each view, which now need to be combined. We
224 first flatten each image embedding into a one-dimensional
225 vector and then use gated pooling attention as described by
226 Wu et al. [37]. Given the individual image embeddings V_i ,

gated pooling attention learns a single embedding:

$$V = \sum_{i=1}^N \alpha_i V_i \quad (1) \quad 228$$

in which α_i are weights for the i th image such that
 $\sum_{i=1}^N \alpha_i = 1$ that are calculated using:

$$\alpha_i = \frac{\exp\{w^T(\tanh(ZV_i^T) \otimes \text{sigm}(GV_i^T))\}}{\sum_{j=1}^N \exp\{w^T(\tanh(ZV_j^T) \otimes \text{sigm}(GV_j^T))\}} \quad (2) \quad 231$$

where $w \in \mathbb{R}^K$, $Z \in \mathbb{R}^{K \times M}$, $G \in \mathbb{R}^{K \times M}$, $M = S_I H_I$,
and K is a hyperparameter we set to 128. Gated pooling
attention introduces non-linearity which helps pool visual
information across the image. With this combined image
embedding $V \in \mathbb{R}^{S_I \times H_I}$, we then project this embedding
to match the embedding dimension H_T of the text embed-
ding so that we can concatenate the text and image embed-
ding together with dimension $\mathbb{R}^{(S_T + S_I) \times H_I}$, where S_T is
the sequence length of the text embedding. This concate-
nated, multimodal embedding is then inputted into the LM
to generate answer text.

3.2. Language Model

243 To mitigate the computational and inference costs of our
244 vision-language model, we aim to use more lightweight
245 LMs with less than one billion parameters. To achieve this,
246 we use two different pre-trained versions of the T5 LM
247 model: T5-Base, which contains around 223 million param-
248 eters, and an 8-bit quantized version of T5-Large ($\approx 750M$
249 parameters). Using these pre-trained LMs, we perform fine-
250 tuning to adapt the LM to the concatenated multi-view im-
251 age and text embeddings. In our experimentation, we found
252 that fine-tuning the whole model for T5-Base works best,
253 but for the quantized T5-Large we use LoRA-Fine-Tuning-
254 Aware Quantization [22], which helps minimize quantiza-
255 tion error with the initialization of LoRA weights.

3.3. Training Process

257 To train EM-VLM4AD, we use the DriveLM dataset [31],
258 the most recent and comprehensive dataset for autonomous
259 driving multi-view VQA with questions related to safety
260 tasks such as perception, planning, prediction, and ego-
261 vehicle behavior prediction. We use the training split of
262 the DriveLM dataset, which contains 656 different scenes
263 from NuScenes [4], 4,072 different multi-view frames, and
264 377,983 different multi-view/QA pairs. To evaluate our ap-
265 proach, we use a 90%/5%/5% split of the traffic scenes from
266 DriveLM so we can evaluate how our model performs on
267 unseen situations. Rather than train all components of our
268 model in one stage, we use a two-stage approach as shown
269 by Figure 1:
270

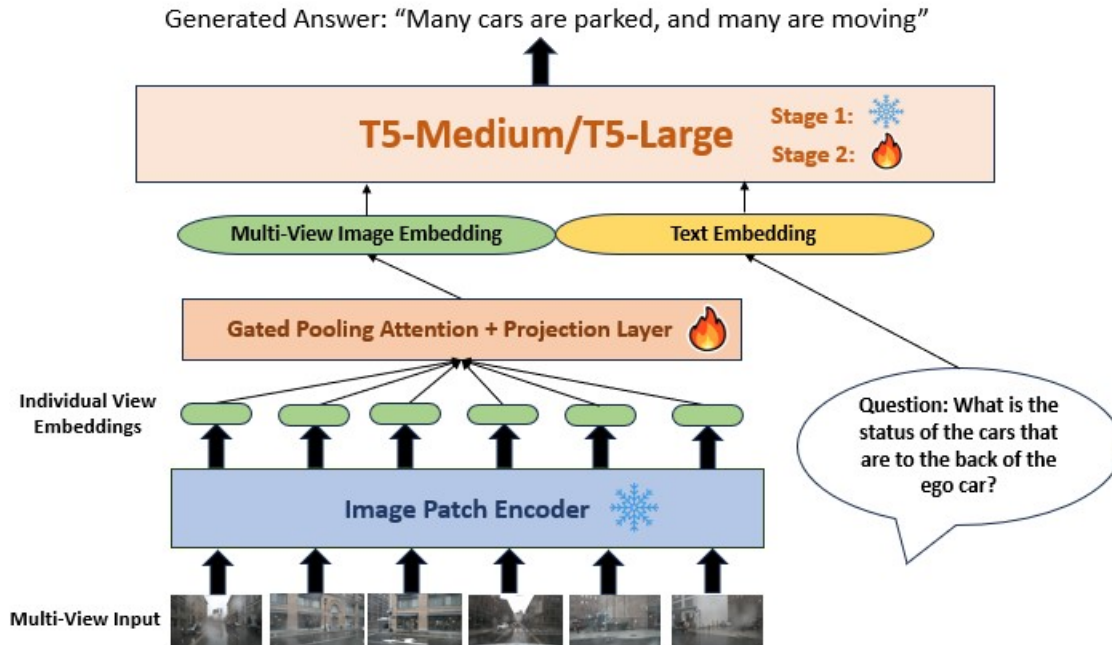


Figure 1. The diagram our model uses to respond to multi-view image input and question prompts. The T5 LM is frozen during Stage 1 of training so the image embedding network learns to align with the T5 embeddings. The image patch encoder is frozen throughout all stages of training, and the Gated Pooling Attention and Projection Layer is trained in both stages.

- In the first stage, we first freeze the image patch encoder and the LM and only train the gated pooling attention and projection layer. This forces the multi-view image embeddings to align with the type of embeddings the LM expects.
- Then in the last stage, we only keep the image patch encoder frozen and start to finetune the LM.

In summary, the image patch encoder is always frozen to maintain generalized image information gathered from pretraining, the gated pooling attention and projection layer is always trained, and the Language Model is only finetuned during the last stage of training.

We perform each training stage for six epochs, which takes around 2.5 days to finish for each model. We use a NVIDIA RTX 3090 Ti to train the T5-Large version of EM-VLM4AD and a V100 Google Colab instance to train EM-VLM4AD with T5-Base. We note that our models can be fit into a single T4 GPU instance, which allows to evaluate these models for free with Google Colab. For hyperparameters, we use a learning rate of $1e-4$, weight decay of 0.05, an exponential learning rate scheduler, and a batch size of 4 for both approaches.

4. Experiments

This section presents an analysis of the quantitative, qualitative, and computational performance of EM-VLM4AD. We use the following metrics commonly used in image cap-

tioning tasks to assess the quality of the model-generated answers:

- BLEU-4 [26]: Measures how many 4-grams in the generated text match those in the reference text.
- ROUGE-L [23]: Calculates sentence similarity scores using the longest common sub-sequence between the generated text and ground-truth text.
- METEOR [3]: Considers exact matches, stemming, synonymy, and word order to measure alignment between model outputs and references.
- CIDEr [34]: To account for lexical and semantic similarity between the generated and reference text, CIDEr weights n-grams with their corresponding TF-IDF weight. This helps de-emphasize n-grams that commonly occur across all examples that may not have important meaning.

For computational analysis, we aim to analyze the memory and computational efficiency of our model, essential aspects in real-time systems where resource constraints exist and inference efficiency is paramount.

4.1. Quantitative Results

We evaluate the BLEU-4, ROUGE-L, METEOR, and CIDEr scores using the test set of unseen traffic scenes we create. Currently, the only existing approach on the DriveLM dataset is DriveLM-Agent [31], which is a finetuned version of BLIP-2. Since this model is not yet public and

Question: What actions could the ego vehicle based on <c2, CAM_FRONT_RIGHT, 378.3, 502.5>? Why take this action and what's the probability?
Prediction: The action is keep going at the same speed. The reason is that there is no safety issue, and the probability is high.
Ground Truth: The action is keep going at the same speed. The reason is that there is no safety issue, and the probability is high.

Question: Are there parked trucks to the back right of the ego car?
Prediction: Yes.
Ground Truth: Yes.

Question: What are the objects to the back left of the ego car?
Prediction: There are many cars **and one truck**, and one pedestrian to the back left of the ego car.
Ground Truth: There are many cars, one truck, and one pedestrian to the back left of the ego car.

Question: Would <c1, CAM_BACK, 761.7, 505.8> be moving in the direction of the ego vehicle?
Prediction: No.
Ground Truth: No.

Question: What is the status of the pedestrian that is to the front left of the ego car?
Prediction: One pedestrian to the front left of the ego car is moving.
Ground Truth: The pedestrian to the front left of the ego car is moving.

Question: What is the future state of <c1, CAM_BACK, 815.0, 516.7>?
Prediction: Keep going straight.
Ground Truth: Keep going straight.

Question: What is the moving status of object <c3, CAM_FRONT_LEFT, 649.2, 649.2>?
Prediction: Going ahead.
Ground Truth: Going ahead.

Question: What will affect driving judgement in this scene?
Prediction: Water droplets on the glass will affect visibility.
Ground Truth: Water droplets on the glass will affect visibility.

Figure 2. Example correct answer generations from EM-VLM4AD. As shown these in these examples, our model is able to perform VQA for various autonomous driving tasks such as perception, planning, and traffic agent behavior prediction.

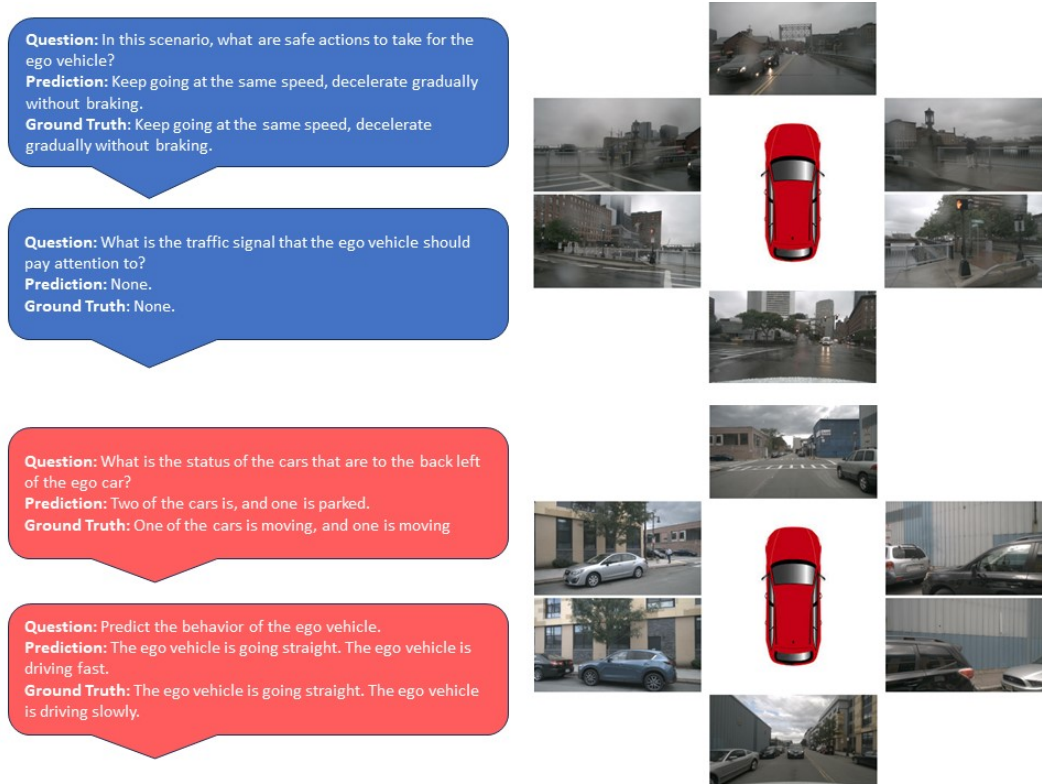


Figure 3. More example generations from EM-VLM4AD. As shown by the red QA examples, EM-VLM4AD can sometimes struggle with grammatical semantics and questions related to ego-vehicle behavior prediction, which may require video input for improved performance.

Model	BLEU-4 \uparrow	METEOR \uparrow	ROUGE-L \uparrow	CIDEr \uparrow
EM-VLM4AD _{Base}	68.73	48.11	81.43	3.96
EM-VLM4AD _{Q-Large}	67.86	47.64	81.00	3.90
DriveLM-Agent [31]	53.09	36.19	66.79	2.79

Table 1. Qualitative comparison of generated answers between DriveLM-Agent and EM-VLM4AD on their respective test sets. EM-VLM4AD_{Base} uses a T5-Base LM backbone, while EM-VLM4AD_{Q-Large} uses an 8-bit quantized T5-Large backbone. Both models outperform DriveLM-Agent in all statistics.

we do not have the computational resources to perform full-precision LoRA training of BLIP-2, we benchmark our approach using the results Sima et al. [31] provide on their private evaluation set. The results from Table 1 demonstrate how both versions of EM-VLM4AD outperform DriveLM-Agent on all metrics, despite having at least 3 billion less model parameters. Out of all three models, the version of EM-VLM4AD that uses T5-Base is the top-performing model.

The superior performance of EM-VLM4AD with the T5-Base backbone over the 8-bit quantized T5-Large version can be attributed to the former’s ability to train a larger parameter set. This facilitates a better adaptation of the language model to the input vision-language embeddings. Conversely, the LoRA finetuning approach for the

8-bit quantized T5-Large LM only changes 3.4% of the network’s weights. While we did try full finetuning for the quantized LM, this over fine-tuned the LM and caused mode collapse.

The integration of multiple frames is a critical advantage that contributes to EM-VLM4AD’s performance versus DriveLM-Agent. Unlike DriveLM-Agent, which only uses the front-view frame as input, our model successfully aggregates information across multiple views with our custom multi-view embedding network. Furthermore, while certain tasks done by LMs are defined as *emergent*, requiring larger models for sufficient results, our study underscores that learning to perform VQA on the DriveLM dataset can be done without increasing model complexity. Therefore, simply adding model complexity may not result

Model	Pretrained Models Used	# of Parameters ↓	FLOP Count ↓	Memory (GB) ↓
EM-VLM4AD _{Base}	T5-Base, ViT-b/32 patch embedder	235M	9.47B	0.94
EM-VLM4AD _{Q-Large}	T5-Large, ViT-b/32 patch embedder	769M	31.5B	0.77
DriveLM-Agent [31]	BLIP-2	3.96B	439B	14.43
DriveMLM [35]	LLaMA-7B, Vit-g/14	8.37B	535B	36
LLM-Driver [5]	LLaMA-7B	7B	268B	28
Drive-GPT4 [38]	LLaMA 2, CLIP	7.3B	329B	29.2

Table 2. Computational comparison of other LMs for Autonomous Driving with both versions of EM-VLM4AD. The EM-VLM4AD models have the smallest number of parameters, memory space, and FLOP count, making them the most efficient and computationally efficient VLM for autonomous driving.

353 in optimal improvements for this specific task.

354 4.2. Computational Analysis

355 We also perform computational analysis to see how EM-
356 VLM4AD compares to other multimodal LMs for au-
357 tonomous driving. Specifically, we focus on three key com-
358 putational metrics: the # of parameters, # of Floating Point
359 Operations (FLOPs), and memory in gigabytes (GB). For
360 these methods, the image encoder and LM constitute the
361 most computationally expensive aspects of these models,
362 so we only focus on these two aspects when calculating
363 these metrics. To estimate the FLOP count for each of these
364 models, we use the `fvcore FLOP counter` module on ex-
365 amples from the DriveLM dataset with a A100 GPU. For
366 the methods we compare to, we add the FLOPs of the
367 image encoder and LM together. The results in Table 2
368 underscore that EM-VLM4AD is considerably more effi-
369 cient than other methods, requiring less memory, computa-
370 tions, and model parameters. Notably, EM-VLM4AD with
371 the T5-Base backbone has the least parameters and FLOP
372 count, while EM-VLM4AD with the T5-Large backbone
373 has the least memory requirements since model weights are
374 only stored in 8 bits. These optimized model design choices
375 enable EM-VLM4AD to provide fast inference times and
376 require less computational resources, critical attributes for
377 any LM implemented for real-time scenarios.

378 4.3. Qualitative Results

379 Figures 2 and 3 showcase some selected multi-frame an-
380 swer generations produced by EM-VLM4AD. Our model
381 can accurately respond to a variety of questions related to
382 perception, traffic agent behavior identification, planning
383 safe ego-vehicle behavior, and identifying important traffic
384 elements in a scene. Through leveraging the general knowl-
385 edge from the pretrained patch embedding network and T5-
386 LM, our system can answer a wide spectrum of questions
387 that encapsulate an end-to-end autonomous driving system.
388 Additionally, EM-VLM4AD demonstrates the ability to un-
389 derstand the c-tag format employed by DriveLM, which en-

codes traffic objects as $\langle c, CAM, x_{pos}, y_{pos} \rangle$. Moreover, 390
this model learns to intelligently extract the most relevant 391
frames for each question, making it an effective multi-frame 392
VLM system. However, EM-VLM4AD exhibits two spe- 393
cific weaknesses: grammatical issues and issues answer- 394
ing questions related to behavior. EM-VLM4AD can oc- 395
casionally generate answers with grammatical errors, hin- 396
dering someone to understand the answer to a question. 397
Adding training techniques such as distillation [17] with 398
larger vision-language models, which have a better under- 399
standing of grammar rules, will help this smaller model 400
learn these complex rules. EM-VLM4AD also struggles 401
with behavior related questions, where the prompt is “Pre- 402
dict the behavior for the ego vehicle”. Adding temporal 403
context through inputting multi-view videos to our network 404
would improve results on this type of question, since be- 405
havior related questions often need more than one frame to 406
make accurate predictions. 407

5. Conclusion 408

We introduce EM-VLM4AD, a lightweight multi-frame 409
vision-language model designed for Visual Question An- 410
swering across various autonomous driving tasks. Com- 411
pared to other LMs tailored for autonomous driving, EM- 412
VLM4AD exhibits notable advantages in terms of mem- 413
ory efficiency and computational requirements, and out- 414
performs the reported scores of DriveLM-Agent in BLEU- 415
4, METEOR, ROUGE, and CIDEr metrics on a DriveLM 416
test dataset. EM-VLM4AD demonstrates proficiency in re- 417
sponding to a variety of autonomous driving questions and 418
dynamically focuses on relevant camera views through our 419
gated pooling attention layer, which effectively integrates 420
view embeddings. In future research, we aspire to evolve 421
our model into a video-language model capable of gener- 422
ating responses from multi-view video inputs, thereby en- 423
hancing EM-VLM4AD’s ability to handle temporal-related 424
inquiries. Furthermore, incorporating multimodal retrieval 425
augmented generation to provide context can enable our 426
model to extract insights from analogous traffic scenar- 427
ios. 428

References

- 429
430
431
432
433
434
435
436
437
438
439
440
441
442
443
444
445
446
447
448
449
450
451
452
453
454
455
456
457
458
459
460
461
462
463
464
465
466
467
468
469
470
471
472
473
474
475
476
477
478
479
480
481
482
483
484
485
- [1] Jean-Baptiste Alayrac, Jeff Donahue, Pauline Luc, Antoine Miech, Iain Barr, Yana Hasson, Karel Lenc, Arthur Mensch, Katherine Millican, Malcolm Reynolds, et al. Flamingo: a visual language model for few-shot learning. *Advances in Neural Information Processing Systems*, 35:23716–23736, 2022. 2
- [2] Ebtesam Almazrouei, Hamza Alobeidli, Abdulaziz Alshamsi, Alessandro Cappelli, Ruxandra Cojocaru, M erouane Debbah,  tienne Goffinet, Daniel Hesslow, Julien Launay, Quentin Malartic, Daniele Mazzotta, Badreddine Noune, Baptiste Pannier, and Guilherme Penedo. The falcon series of open language models, 2023. 2
- [3] Satanjeev Banerjee and Alon Lavie. Meteor: An automatic metric for mt evaluation with improved correlation with human judgments. In *Proceedings of the acl workshop on intrinsic and extrinsic evaluation measures for machine translation and/or summarization*, pages 65–72, 2005. 4
- [4] Holger Caesar, Varun Bankiti, Alex H Lang, Sourabh Vora, Venice Erin Liong, Qiang Xu, Anush Krishnan, Yu Pan, Giancarlo Baldan, and Oscar Beijbom. nuscenes: A multi-modal dataset for autonomous driving. In *Proceedings of the IEEE/CVF conference on computer vision and pattern recognition*, pages 11621–11631, 2020. 2, 3
- [5] Long Chen, Oleg Sinavski, Jan H unermann, Alice Karnsund, Andrew James Willmott, Danny Birch, Daniel Maund, and Jamie Shotton. Driving with llms: Fusing object-level vector modality for explainable autonomous driving. *arXiv preprint arXiv:2310.01957*, 2023. 1, 2, 7
- [6] Jaemin Cho, Jie Lei, Hao Tan, and Mohit Bansal. Unifying vision-and-language tasks via text generation. In *International Conference on Machine Learning*, pages 1931–1942. PMLR, 2021. 2
- [7] Wenliang Dai, Junnan Li, Dongxu Li, Anthony Meng Huat Tiong, Junqi Zhao, Weisheng Wang, Boyang Li, Pascale Fung, and Steven Hoi. Instructblip: Towards general-purpose vision-language models with instruction tuning, 2023. 2
- [8] Jia Deng, Wei Dong, Richard Socher, Li-Jia Li, Kai Li, and Li Fei-Fei. Imagenet: A large-scale hierarchical image database. In *2009 IEEE conference on computer vision and pattern recognition*, pages 248–255. Ieee, 2009. 3
- [9] Jacob Devlin, Ming-Wei Chang, Kenton Lee, and Kristina Toutanova. Bert: Pre-training of deep bidirectional transformers for language understanding. *arXiv preprint arXiv:1810.04805*, 2018. 2
- [10] Alexey Dosovitskiy, Lucas Beyer, Alexander Kolesnikov, Dirk Weissenborn, Xiaohua Zhai, Thomas Unterthiner, Mostafa Dehghani, Matthias Minderer, Georg Heigold, Sylvain Gelly, et al. An image is worth 16x16 words: Transformers for image recognition at scale. *arXiv preprint arXiv:2010.11929*, 2020. 2, 3
- [11] Yifan Du, Zikang Liu, Junyi Li, and Wayne Xin Zhao. A survey of vision-language pre-trained models. *arXiv preprint arXiv:2202.10936*, 2022. 2
- [12] Zhiyuan Fang, Jianfeng Wang, Xiaowei Hu, Lijuan Wang, Yezhou Yang, and Zicheng Liu. Compressing visual linguistic model via knowledge distillation. In *Proceedings of the IEEE/CVF International Conference on Computer Vision*, pages 1428–1438, 2021. 2
- [13] Ross Greer and Mohan Trivedi. Towards explainable, safe autonomous driving with language embeddings for novelty identification and active learning: Framework and experimental analysis with real-world data sets. *arXiv preprint arXiv:2402.07320*, 2024. 2
- [14] Ross Greer, Akshay Gopalkrishnan, Jacob Landgren, Lulua Rakla, Anish Gopalan, and Mohan Trivedi. Robust traffic light detection using salience-sensitive loss: Computational framework and evaluations. In *2023 IEEE Intelligent Vehicles Symposium (IV)*, pages 1–7. IEEE, 2023. 1
- [15] Ross Greer, Bj ork Antoniussen, Mathias V Andersen, Andreas M ogelmoose, and Mohan M Trivedi. The why, when, and how to use active learning in large-data-driven 3d object detection for safe autonomous driving: An empirical exploration. *arXiv preprint arXiv:2401.16634*, 2024. 500
- [16] Ross Greer, Akshay Gopalkrishnan, Maitrayee Keskar, and Mohan M Trivedi. Patterns of vehicle lights: Addressing complexities of camera-based vehicle light datasets and metrics. *Pattern Recognition Letters*, 178:209–215, 2024. 1
- [17] Geoffrey Hinton, Oriol Vinyals, and Jeff Dean. Distilling the knowledge in a neural network. *arXiv preprint arXiv:1503.02531*, 2015. 7
- [18] Edward J Hu, Yelong Shen, Phillip Wallis, Zeyuan Allen-Zhu, Yuanzhi Li, Shean Wang, Lu Wang, and Weizhu Chen. Lora: Low-rank adaptation of large language models. *arXiv preprint arXiv:2106.09685*, 2021. 1, 2
- [19] Jinkyu Kim, Anna Rohrbach, Trevor Darrell, John Canny, and Zeynep Akata. Textual explanations for self-driving vehicles. In *Proceedings of the European conference on computer vision (ECCV)*, pages 563–578, 2018. 2
- [20] Junnan Li, Dongxu Li, Silvio Savarese, and Steven Hoi. Blip-2: Bootstrapping language-image pre-training with frozen image encoders and large language models. *arXiv preprint arXiv:2301.12597*, 2023. 1, 2
- [21] Xuanlin Li, Yunhao Fang, Minghua Liu, Zhan Ling, Zhuowen Tu, and Hao Su. Distilling large vision-language model with out-of-distribution generalizability. In *Proceedings of the IEEE/CVF International Conference on Computer Vision*, pages 2492–2503, 2023. 2
- [22] Yixiao Li, Yifan Yu, Chen Liang, Pengcheng He, Nikos Karampatziakis, Weizhu Chen, and Tuo Zhao. Loftq: Lora-fine-tuning-aware quantization for large language models, 2023. 3
- [23] Chin-Yew Lin. Rouge: A package for automatic evaluation of summaries. In *Text summarization branches out*, pages 74–81, 2004. 4
- [24] Jiageng Mao, Yuxi Qian, Hang Zhao, and Yue Wang. Gpt-driver: Learning to drive with gpt. *arXiv preprint arXiv:2310.01415*, 2023. 1, 2
- [25] Kaouther Messaoud, Nachiket Deo, Mohan M Trivedi, and Fawzi Nashashibi. Trajectory prediction for autonomous driving based on multi-head attention with joint agent-map representation. In *2021 IEEE Intelligent Vehicles Symposium (IV)*, pages 165–170. IEEE, 2021. 1
- 486
487
488
489
490
491
492
493
494
495
496
497
498
499
500
501
502
503
504
505
506
507
508
509
510
511
512
513
514
515
516
517
518
519
520
521
522
523
524
525
526
527
528
529
530
531
532
533
534
535
536
537
538
539
540
541
542

- 543 [26] Kishore Papineni, Salim Roukos, Todd Ward, and Wei-Jing
544 Zhu. Bleu: a method for automatic evaluation of machine
545 translation. In *Proceedings of the 40th annual meeting of the*
546 *Association for Computational Linguistics*, pages 311–318,
547 2002. 4
- 548 [27] Alec Radford, Jeffrey Wu, Rewon Child, David Luan, Dario
549 Amodei, Ilya Sutskever, et al. Language models are unsu-
550 pervised multitask learners. *OpenAI blog*, 1(8):9, 2019. 2
- 551 [28] Alec Radford, Jong Wook Kim, Chris Hallacy, Aditya
552 Ramesh, Gabriel Goh, Sandhini Agarwal, Girish Sastry,
553 Amanda Askell, Pamela Mishkin, Jack Clark, et al. Learning
554 transferable visual models from natural language supervi-
555 sion. In *International conference on machine learning*, pages
556 8748–8763. PMLR, 2021. 2
- 557 [29] Colin Raffel, Noam Shazeer, Adam Roberts, Katherine Lee,
558 Sharan Narang, Michael Matena, Yanqi Zhou, Wei Li, and
559 Peter J. Liu. Exploring the limits of transfer learning with a
560 unified text-to-text transformer, 2023. 2, 3
- 561 [30] Hao Sha, Yao Mu, Yuxuan Jiang, Li Chen, Chenfeng Xu,
562 Ping Luo, Shengbo Eben Li, Masayoshi Tomizuka, Wei
563 Zhan, and Mingyu Ding. LanguageMPC: Large language
564 models as decision makers for autonomous driving, 2023.
565 2
- 566 [31] Chonghao Sima, Katrin Renz, Kashyap Chitta, Li Chen,
567 Hanxue Zhang, Chengen Xie, Ping Luo, Andreas Geiger,
568 and Hongyang Li. Drivelm: Driving with graph visual ques-
569 tion answering. *arXiv preprint arXiv:2312.14150*, 2023. 1,
570 2, 3, 4, 6, 7
- 571 [32] Hugo Touvron, Thibaut Lavril, Gautier Izacard, Xavier
572 Martinet, Marie-Anne Lachaux, Timothée Lacroix, Baptiste
573 Rozière, Naman Goyal, Eric Hambro, Faisal Azhar, et al.
574 Llama: Open and efficient foundation language models.
575 *arXiv preprint arXiv:2302.13971*, 2023. 1, 2
- 576 [33] Ashish Vaswani, Noam Shazeer, Niki Parmar, Jakob Uszko-
577 reit, Llion Jones, Aidan N Gomez, Łukasz Kaiser, and Illia
578 Polosukhin. Attention is all you need. *Advances in neural*
579 *information processing systems*, 30, 2017. 2
- 580 [34] Ramakrishna Vedantam, C Lawrence Zitnick, and Devi
581 Parikh. Cider: Consensus-based image description evalua-
582 tion. In *Proceedings of the IEEE conference on computer*
583 *vision and pattern recognition*, pages 4566–4575, 2015. 4
- 584 [35] Wenhai Wang, Jiangwei Xie, ChuanYang Hu, Haoming Zou,
585 Jianan Fan, Wenwen Tong, Yang Wen, Silei Wu, Hanming
586 Deng, Zhiqi Li, Hao Tian, Lewei Lu, Xizhou Zhu, Xiaogang
587 Wang, Yu Qiao, and Jifeng Dai. Drivelm: Aligning multi-
588 modal large language models with behavioral planning states
589 for autonomous driving, 2023. 2, 7
- 590 [36] Jason Wei, Xuezhi Wang, Dale Schuurmans, Maarten
591 Bosma, Brian Ichter, Fei Xia, Ed Chi, Quoc Le, and Denny
592 Zhou. Chain-of-thought prompting elicits reasoning in large
593 language models, 2023. 2
- 594 [37] Wenyi Wu, Qi Li, Wenliang Zhong, and Junzhou Huang.
595 Mivc: Multiple instance visual component for visual-
596 language models. In *Proceedings of the IEEE/CVF Win-
597 ter Conference on Applications of Computer Vision*, pages
598 8117–8126, 2024. 1, 3
- 599 [38] Zhenhua Xu, Yujia Zhang, Enze Xie, Zhen Zhao, Yong Guo,
600 Kenneth KY Wong, Zhenguo Li, and Hengshuang Zhao.

Drivept4: Interpretable end-to-end autonomous driving via
large language model. *arXiv preprint arXiv:2310.01412*,
2023. 1, 2, 3, 7

601
602
603